

# Analysis of Spatial Variability for the Development of Reduced Lead Body Surface Maps

Frederique J Vanheusden<sup>1</sup>, Xin Li<sup>1</sup>, Gavin S Chu<sup>2</sup>, Tiago P Almeida<sup>1</sup>, G André Ng<sup>2</sup>,  
Fernando S Schlindwein<sup>1,2</sup>

<sup>1</sup>Department of Engineering, University of Leicester, Leicester, UK

<sup>2</sup>Department of Cardiovascular Sciences, Glenfield Hospital, Leicester, UK

## Abstract

*The spatial frequency of measurement points from standard ECG systems lacks accuracy to diagnose local variability in cardiac activity on the torso. Body Surface Mapping (BSM) improves this accuracy, but lacks the simplicity to be implemented in clinic on a regular basis. Reduced-lead BSM system improves applicability, but currently no standardization of lead reduction has been agreed upon. This research investigates the reduction of BSMs based on Lomb-Scargle Spectral Analysis to determine an appropriate electrode positioning through spatial frequency assessment. Based on the measurement of 13 healthy volunteers, a 128 electrode system could be reduced to a 36 electrode system and an 84 electrode system for ventricular and atrial activity measurements, respectively, with up to 10% loss of the full information provided by the original body surface potential map. Further research will investigate the appropriate positions of these electrodes and the effect of lead reduction for various cardiac abnormalities.*

## 1. Introduction

Currently, the standard 12-lead ECG is routinely used for non-invasive cardiac assessment and diagnosis. Due to the limited number of measuring points, however, the ECG does not always provide sufficient diagnostic accuracy for detection of local abnormalities. This hampers the detection and characterisation of local arrhythmias which might be of interest.

Improvements can be made by increasing the number of measurement points on the torso surface. These extended ECG systems are known as body surface mapping (BSM) systems, which offer improved diagnostic accuracy [1]. BSM systems are not routinely implemented in clinic, for the main reasons that the time consumed for application and data interpretation of up to 400 electrodes is outbalanced by standard ECG [1, 2]. To overcome these issues, many research groups have

attempted to reduce the number of leads without losing relevant information. Amongst other techniques, the development of reduced-lead BSM systems based on source ‘generators’ has been investigated with promising result [3, 4]. These techniques find uncorrelated sources from the BSM signals and rank them according to the amount of information that each one of these sources contain. Consequently, sources that represent little information to the original BSM signals can be discarded without significant loss of information.

Due to the variation in BSM systems and different reduced-lead systems solutions, no gold standard has been developed for BSM, which makes comparing results between various research groups challenging [5]. Besides this, especially for the reduced systems, one could argue that their relationship with the original measurements might be misinterpreted. A more classical approach which is directly related to the BSM measurements is the determination of the Nyquist frequency from spatial spectral analysis. The aim of this study is to find the optimum spatial frequency of electrode positioning for reduced-lead BSMs using Lomb-Scargle Spectral Analysis (LSSA) [6].

### 1.1. Lomb-Scargle spectral analysis

In most instances, spectral analysis would be performed with a Fast Fourier Transform (FFT). However, the FFT assumes uniform positioning of the sampling electrodes. Since BSM electrodes are usually positioned non-uniformly over the torso, LSSA was used to determine the spatial Nyquist frequency. The LSSA periodogram for  $N$  samples at  $h_j, j = 1, 2, \dots, N$  can be calculated as follows [7]:

$$P_N(\omega) = \frac{1}{2\sigma^2} \cdot \left\{ \frac{[\sum_j (h_j - \bar{h}) \cos \omega(t_j - \tau)]^2}{\sum_j \cos^2 \omega(t_j - \tau)} + \frac{[\sum_j (h_j - \bar{h}) \sin \omega(t_j - \tau)]^2}{\sum_j \sin^2 \omega(t_j - \tau)} \right\} \quad (1)$$

In this formula,  $\bar{h}$  defines the average of the signal at  $h$ , and  $\sigma^2$  is the variance of the signal: The offset  $\tau$  is added to make the periodogram independent of shifting all time

samples by a constant. This offset is calculated using:

$$\tan(2\omega\tau) = \frac{\sum_j \sin 2\omega t_j}{\sum_j \cos 2\omega t_j} \quad (2)$$

## 2. Methods

BSM measurements were taken from 13 healthy volunteers using a 128-electrode ActiveTwo BSM system (BioSemi, Netherlands) set up as shown in Figure 1. For each subject, two measurements of one minute, with a break of 2 minutes, were recorded at a rate of 2048 Hz. The Wilson Central Terminal, indicated as individual electrodes in Figure 1, was used as reference. Raw data were analysed in Matlab R2012b (The Mathworks Inc., Nattick, Massachusetts, USA). Prior to analysis, signals were band-pass filtered between 0.16 Hz and 50 Hz using a second order Bessel filter. Afterwards, signals were visually inspected and discarded in case of excessive noise.

### 2.1. Reduced-lead BSM using LSSA

To find the optimum spatial frequency, LSSA was performed individually in horizontal (latitudinal) and vertical (longitudinal) directions, creating a 2D representation of electrode density. This density could then be translated in a matrix formula of  $N$  horizontal-by- $M$  vertical electrodes. For this purpose, the electrodes were separated in 8 horizontal layers containing 16 electrodes, and 16 vertical layers of 8 electrodes. The distance between the individual electrodes was measured, considering the electrode which was on the left bottom of the chest as the origin (Figure 2A).

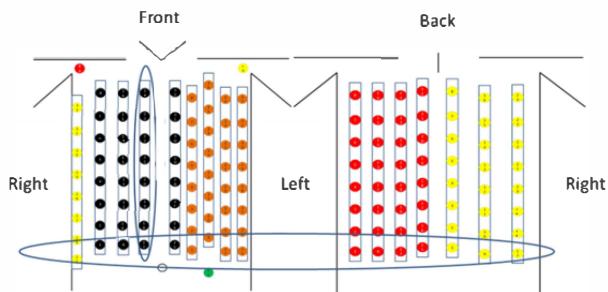


Figure 1. Standard setup of the 128-electrode BSM system. Electrode strips are indicated with rectangles. The WCT electrodes are shown as individual circles on the extremities. The system's offset is measured by the central electrodes. The vertical and horizontal ellipses show how the longitude and latitude are defined, respectively, for Lomb periodogram analysis.

Analysis was focused individually on ventricular activation (QRS complex) and atrial activity. For ventricular activity analysis, the QRS complex was segmented as suggested by Salinet *et al* [8]. These intervals were then down-sampled to 200 Hz (Figure 2B).

The signals of each electrode layer were then represented as voltage over distance according each electrode position each time sample (Figure 2C).

From each distance-voltage plot, the LSSA was calculated using a modified version of the algorithms suggested by Press *et al.* implemented in Matlab [7]. The ratio of signal described by subsets of the total 128-lead BSM system and the 'total' signal were calculated based on the area under curve (AUC) of the spectrum (Figure 2D). In these calculation, a noise threshold was considered, which removed all peaks in the spectrum which were smaller than 6 decibels (dB) of the maximum probability, as suggested by Evans *et al.* [9]. The average AUC for each spatial frequency in all samples was then determined.

For analysing atrial activity, the QRST segments found for each patient were subtracted according to [8]. LSSA was then performed as described above, but by analysing 1s long windows of atrial activity with 25% overlap instead of specific complexes.

To consider the effects of using FFT instead of LSSA, all voltage-distance plots within 3s (25% overlap) of the original ECG signal were analysed. Secondly, the FFT was also calculated for the QRS complexes.

### 2.2. Reconstruction of reduced-lead maps

Reduced-lead maps were reconstructed for the average Nyquist frequency found for all subjects during the 3s full-ECG and QRS complex windows. Electrodes were spread uniformly over the torso. The total BSM map was estimated using linear interpolation.

## 3. Results

### 3.1. Reduced-lead BSM from LSSA

The results of the LSSA and FFT for spatial frequency analysis of an individual strip over three different 3s windows are shown in Figure 3. Samples with high power frequency components are indicated with ellipses. The ECGs of the windows were plotted for visualizing the correlation with the spectra. After analysis of the processed BSM signals, the LSSA showed a remarkable high power of spatial frequencies at about  $0.0065 \text{ mm}^{-1} \pm 0.0006 \text{ mm}^{-1}$ , which would suggest an 8x8 grid (64 electrodes in total). This maximal power changed during QRS peak to  $0.0035 \text{ mm}^{-1} \pm 0.0004 \text{ mm}^{-1}$  (36 electrodes). The power value also significantly increased, as is especially visible on the FFT spectrum.

From this, it could also be observed that the FFT analysis might hide important information. For this purpose, AUC analysis was performed only on LSSA data. Figure 4 shows the percentage to the total BSM signal represented by a reduced-lead BSM for ventricular

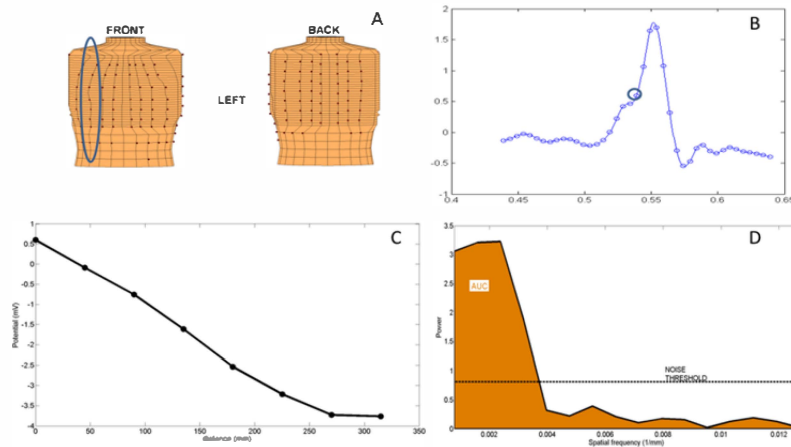


Figure 2. An overview of the Lomb analysis to determine the spatial frequency during ventricular activation. For each of the electrodes on one latitude or longitude (2A), the QRS complex is segmented and down-sampled (2B). From each sample (e.g. indicated spot on 2B), the voltages measured at all electrodes on the latitudinal/longitudinal strip are plotted over distance (2C). From this, the frequency spectrum is calculated. After applying a noise threshold (black box), the AUC of the spectrum was calculated (2D).

and atrial activity. The graph represents the mean AUC determined over all patients for all samples.

Finally, maps with reduced leads were reconstructed. One example for 36- and 64-electrode systems is compared to the original map in Figure 5. Correlation coefficients for reconstructed maps varied widely between  $0.54 \pm 0.07$  and  $.61 \pm 0.07$  for 36- and 64-electrode systems, respectively.

#### 4. Discussion

For all subjects, a maximum of five electrodes showed signals with excessive noise after processing. It was decided to discard these signals from further processing rather than performing an interpolation.

A remarkable difference in FFT and Lomb spectra was found during the analysis of the spatial frequency. This shows that the FFT, due to the assumption of uniform spacing, is probably unable to show possibly important spectral information. The reduction in most significant frequency during QRS intervals can be explained by the improved signal-to-noise ratio during this interval.

Before determining the AUC of the Lomb spectra, a threshold was applied to remove low-power peaks [9]. By considering this threshold, and averaging all spectra for all patients, it could be shown that a reduction of the amount of electrodes to 36 (6-by-6 system) would allow capturing about 90% of the total signal for ventricular activity. For atrial activity, about 84 electrodes (13-by-7 system) would be necessary for representing about 90% of the captured cardiac activity. One reason for this might be that the signal-to-noise ratio during QRS is higher than during atrial activity, which allows the noise threshold to better discard high-frequency components.

From the reconstructed maps, it could be observed that the general shape of the BSM was maintained. The

correlation coefficients, however, showed quite low correlations with the original map. The main factor is assumed to be the uniform positioning of electrodes. It is therefore concluded that the LSSA analysis could be a starting point for estimating the amount of electrodes needed to reproduce accurate maps. The best position of these electrodes will need to be determined with an alternative strategy.

From the starting point perspective, one could argue that a starting setup of 128 electrodes might be insufficient for correctly representing BSMs. Similar research could however be performed on higher-resolution systems for comparison.

Another issue is to determine where the reduced-lead BSM electrodes should be positioned. From a clinical perspective, a well-structured electrode system would be preferred. It is however known that non-uniform electrode positioning allows for better BSM representations [10]. Future research will be focusing on comparisons between different reduced-lead algorithms proposed (e.g. [3] and [4]). Furthermore, activities will be focused on reducing BSM for different cardiac abnormalities to determine how these affect lead reduction.

#### 5. Conclusion

The effect of lead-reduction on the information content of a BSM was investigated. It was shown that, starting with a 128 electrode system, during ventricular activation, 36 electrodes would be sufficient to describe circa 90% of total BSM information. For measuring atrial activity at this detail, 84 electrodes would be sufficient. Future research will investigate the optimal positioning of these electrodes, as well as the possibility for lead reduction in various cardiac abnormalities.

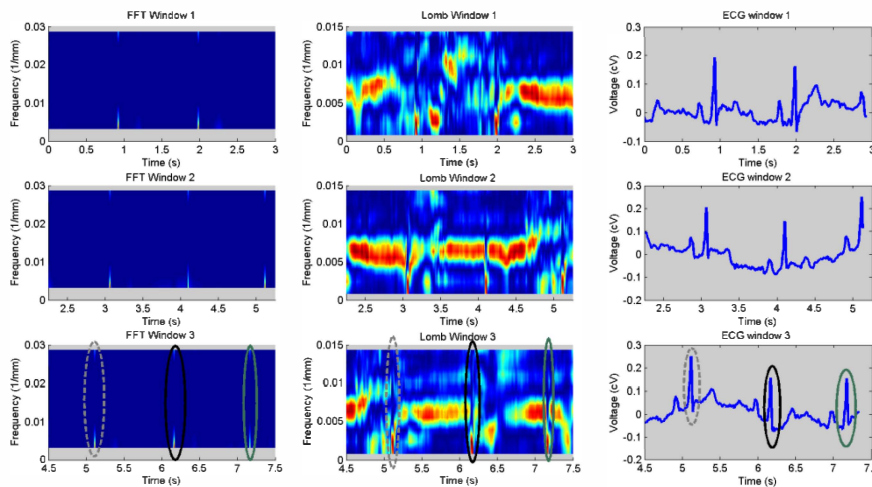


Figure 3. A comparison between the FFT and Lomb spatial spectra for one strip over three different 3s windows. The ECG output of one of the electrodes is given for orientation (right). High power frequencies regions are coloured in red. The position of the QRS complexes in the spectrograms is given for the third window. A reduction in the spatial frequency spectra during these QRS time intervals can be seen in the Lomb spectra. Left: FFT. Middle: LSSA.

## Acknowledgements

The authors would like to thank the EMPF and IPEM for supporting this research. F. Vanheusden is funded by the Leicester Cardiovascular Biomedical Research Unit. T. Almeida is funded by CNPq (Brazil, Grant N 200251/2012-0). This study is part of the research portfolio supported by the NIHR Leicester Cardiovascular Biomedical Research Unit.

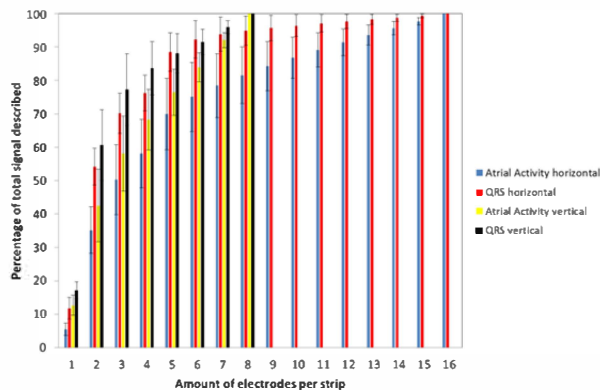


Figure 4. Estimation (mean  $\pm$  SD) of the amount of BSM information retained after LSSA lead reduction for all patients.

## References

- [1] Taccardi B, Punske B, Lux R, *et al.*. Useful lessons from body surface mapping. *J Cardiovasc Electrophys* 1998;9:773-786.
- [2] Punske B. Noninvasive electrical imaging: is it ready for clinical application. *J Cardiovasc Electrophys* 2003;14:720-721.
- [3] Barr R, Spach M, Herman-Giddens G. Selection of the number and positions of measuring locations for Electrocardiography. *IEEE Trans Biomed Eng* 1971;18:125-138.

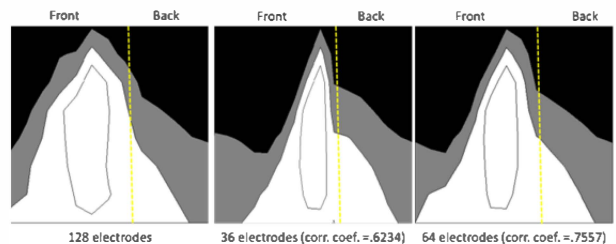


Figure 5: Example of reproduced BSMs during QRS peak. The correlation coefficient (corr. coef.) is indicated. Contours are drawn every 0.5 mV.

- [4] Finlay D, Nugent C, Donnelly M, *et al.*. Selection of optimal recording sites for lead body surface potential mapping: A sequential selection based approach. *BMC Med Inf Decis Mak* 2006;6:1-9.
- [5] Hoekema R, Uijen G, Stilli D, *et al.*. Lead system transformation of body surface map data *J Electrocardiol* 1998;31:71-82.
- [6] Scargle J. Studies in astronomical time series analysis II. Statistical aspects of spectral analysis of unevenly spaced data. *Astrophys J* 1982;263:835-853.
- [7] Press W, Teukolsky S, Vetterling W, *et al.*. Numerical recipes in C. Cambridge University: Cambridge, UK 1992;575-584.
- [8] Salinet J, Madeiro J, Cortez P, *et al.*. Analysis of QRS-T subtraction in unipolar atrial fibrillation electrograms. *Med Biol Eng Comput* 2013 (in press).
- [9] Evans D, Schlindwein F, Levene M. An automatic system for capturing and processing ultrasonic Doppler signals and blood pressure signals. *Clin Phys Physiol Meas* 1989;10:241-251.
- [10] Hoekema R, Uijen G, van Oosterom A. On selecting a body surface mapping procedure. *J Electrocardiol* 1999;32:93-101.

Address for correspondence:  
 Frederique Vanheusden, Department of Engineering  
 University of Leicester, University Road,  
 Leicester, LE1 7RH, United Kingdom.  
 fjv2@le.ac.uk